Timing-jitter reduction in a dispersion-managed soliton system

R.-M. Mu, V. S. Grigoryan, C. R. Menyuk, E. A. Golovchenko,* and A. N. Pilipetskii*

Department of Computer Science and Electrical Engineering, University of Maryland Baltimore County, Baltimore, Maryland 21250

Received December 15, 1997

We found by using Monte Carlo simulations that the timing jitter in a dispersion-managed soliton system decreases as the strength of the dispersion management and hence the ratio of the pulse energy to the pulse bandwidth increases. The results are in qualitative but not quantitative agreement with earlier predictions that the decrease is inversely proportional to the square root of the pulse energy. Using an improved semi-analytical theory, we obtained quantitative agreement with the simulations. © 1998 Optical Society of America

OCIS codes: 060.5530, 060.2330.

Dispersion management is a promising approach for minimizing the jitter of the pulse arrival time in a soliton system[1–4] that is due to the Gordon–Haus effect.[5] Dispersion-managed solitons periodically spread and recompress in a dispersion-managed system, returning to the same initial shape after propagating one period through the dispersion map. Thus their shape is not continually stationary, as is the case for standard solitons, but is only periodically stationary. The spreading that occurs during the propagation effectively lowers the nonlinearity so that the energy of a dispersion-managed soliton with a given average dispersion is higher than for standard solitons and increases with the strength of the dispersion management by an amount that is referred to as an enhancement factor.[6,7] Since the timing jitter is inversely proportional to the soliton amplitude in a standard soliton system, it is natural to anticipate that the timing jitter will be (at least roughly) inversely proportional to the square root of the enhancement factor, and both theoretical and experimental studies to date support this hypothesis.[2–4] However, the shape of the dispersion-managed soliton at its point of maximum compression changes and its time–bandwidth product grows as the strength of the dispersion management increases.[7] Thus it would be surprising if the timing jitter were reduced by exactly the square root of the enhancement factor. In this Letter we carry out a set of careful Monte Carlo simulations, and we show that the reduction can be significantly less—as much as 30% in one case that we examined. We also compare the simulations with a semi-analytical theory based on linearizing the noise contribution about the numerically determined pulse shape and find excellent agreement.

The use of linearization in this context is highly significant. Linearization was used by other authors[5–11] to calculate the effects of amplified-spontaneous-emission (ASE) noise. However, in all this research a fixed, analytically determined signal shape before linearization was assumed. More recently, Kumur and Lederer[12] and Georges *et al.*[13] considered the timing jitter of dispersion-managed solitons, using a quadratic *ansatz* for the pulse chirp. In real systems the pulse evolution is usually too complex to be captured in a simple *ansatz*, but, on the other hand, the ASE noise contribution is often small so that linearization is valid. Thus, our approach of linearizing around numerically determined pulse shapes seems likely to have broader applicability than just to the case considered in this Letter as a way of avoiding numerically time-consuming Monte Carlo simulations.

We considered a dispersion-managed soliton transmission system with lumped amplifiers and a periodic dispersion map that is described by the perturbed nonlinear Schrödinger equation, which we write in the form

$$i\,\frac{\partial u}{\partial z} + \frac{1}{2}\,D(z)\,\frac{\partial^2 u}{\partial t^2} + \gamma|u|^2 u = ig(z)u + \hat{F}(z,t)\,, \quad (1)$$

where we use a notation introduced by Haus[14] that is well adapted to the study of noise effects. We retain t as unnormalized time, and the intensity $|u|^2$ is normalized to the photon flow. The distance variable z corresponds to the physical distance multiplied by the absolute value of the path-average dispersion $|\overline{\beta''}|$. The dispersion coefficient $D(z)$ equals $-\beta''(z)/|\overline{\beta''}|$, where $\beta''(z)$ is the local dispersion. The nonlinear coefficient γ equals $2\pi h\nu^2 n_2/cA_{\text{eff}}|\overline{\beta''}|$, where ν is the carrier frequency, n_2 is the Kerr coefficient, and c is the speed of light in vacuum. The distributed gain coefficient $g(z)$ equals the amplitude gain g_0 at the amplifiers and equals the loss $-\Gamma < 0$ elsewhere; $g(z)$ integrates to zero over one amplifier period. The contribution of the ASE noise $\hat{F}(z,t)$ is delta correlated:

$$\langle \hat{F}(z,t)\hat{F}^*(z',t')\rangle = 2\theta(z)g_0\delta(z-z')\delta(t-t')\,, \quad (2)$$

where for mathematical convenience we set $\theta(z)$ equal to the spontaneous-emission factor n_{sp} at the amplifiers and zero elsewhere so there is no noise contribution outside the amplifiers. We now define the average pulse position t_p:

$$t_p = \frac{1}{U}\int_{-\infty}^{\infty} t|u(t)|^2 \mathrm{d}t\,, \quad (3)$$

where $U = \int_{-\infty}^{\infty}|u(t)|^2\mathrm{d}t$ is the total photon number. We also define the central frequency Ω of $u(z,t)$ as

$$\Omega = \frac{1}{2iU}\int_{-\infty}^{\infty}\left(\frac{\partial u}{\partial t}\,u^* - \frac{\partial u^*}{\partial t}\,u\right)\mathrm{d}t\,. \quad (4)$$

0146-9592/98/120930-03$15.00/0

It is convenient to remove the central frequency from $u(z, t)$ by means of defining $q(z, t) = u(z, t)\exp(-i\Omega t)$. We now find that the standard deviation of t_p can be written as

$$\sigma_t = (\langle {t_p}^2\rangle - \langle t_p\rangle^2)^{1/2} = (A + B + C)^{1/2}, \tag{5}$$

where

$$A = 8\int_0^z \mathrm{d}z_1 D(z_1)\int_0^{z_1}\mathrm{d}z_2 D(z_2)\int_0^{z_2}\frac{\mathrm{d}z_2'}{U^2(z_2')}\,\theta(z_2')g_0 \times\left[\int_{-\infty}^{\infty}\left|\frac{\partial q(z_2', t)}{\partial t}\right|^2\mathrm{d}t\right], \tag{6a}$$

$$B = -4i\int_0^z \mathrm{d}z_1 D(z_1)\int_0^{z_1}\frac{\mathrm{d}z_2}{U^2(z_2)}\,\theta(z_2)g_0 \times\left\{\int_{-\infty}^{\infty}(t - t_p)\left[\frac{\partial q(z_2, t)}{\partial t}\,q^*(z_2, t) - \frac{\partial q^*(z_2, t)}{\partial t}\,q(z_2, t)\right]\mathrm{d}t\right\}, \tag{6b}$$

$$C = 4\int_0^z \frac{\mathrm{d}z_1}{U^2(z_1)}\,\theta(z_1)g_0\left[\int_{-\infty}^{\infty}(t - t_p)^2|q(z_1, t)|^2\mathrm{d}t\right]. \tag{6c}$$

The first term in Eq. (5), A, gives the contribution to the timing jitter from the accumulated frequency shift along the fiber, where the innermost integration gives the individual contribution of each amplifier. This term typically makes the largest contribution to the timing jitter. One can see that the frequency shift depends on both the pulse bandwidth $\int_{-\infty}^{\infty}|\partial q/\partial t|^2\mathrm{d}t/U$ and the photon number U. This term increases proportionally to z^3. The second term, B, gives the contribution to the timing jitter induced by the pulse chirp. Suppose, for example, that $q(z, t)$ is chirped at a particular amplifier, as will generally be the case for dispersion-managed solitons, so that we can write $q = Q\exp(i\alpha t^2)$, where $Q(z, t)$ is symmetric about $t = 0$. In this case the time integral in Eq. (6b) becomes $4\alpha i\int_{-\infty}^{\infty}(t - t_p)^2|Q|^2\mathrm{d}t$, which is proportional to the chirp parameter α. The final term, C, gives the direct contribution of the ASE noise to the timing jitter. Terms A and C appear in the theory of standard solitons and were described, for example, by Haus,[14] whereas the term B is a new factor. Equation (5) is obtained by linearization of Eq. (1) about the pulse shape $u(z, t)$ and solution of the resulting Langevin equation.

We now turn to the calculation of the timing jitter for dispersion-managed solitons by use of both the linearization approach described above and Monte Carlo simulations. In our simulations we solve Eq. (1) by using a standard split-step approach. The effect of the ASE noise contained in the term $\hat{F}(z, t)$ is modeled by addition of noise in the Fourier domain immediately after the amplifiers. Writing the Fourier transform of $u(z, t)$ as $\tilde{u}(z, \omega)$ and integrating Eq. (1), we find that we should add an amount of noise $\delta\tilde{u} = A\exp(i\varphi)$ to each Fourier component, where $A = [n_{\mathrm{sp}}(G - 1)\Delta\nu]^{1/2}$, G is the total gain of the amplifier, φ is a random phase from 0 to 2π, and $\Delta\nu$ is the bandwidth associated with each component. As in Ref. 7, we used a dispersion map consisting of alternating 100-km spans of positive and negative dispersion, and we injected a chirp-free pulse at the midpoint of the negative-dispersion segment with a FWHM duration t_{FWHM} equal to 20 ps. Fiber loss is 0.21 dB/km with an amplifier spacing of 50 km. The fiber effective area A_{eff} is 50 $\mu\mathrm{m}^2$, the Kerr coefficient n_2 is 2.6×10^{-16} cm^2/W, and the spontaneous-emission factor n_{sp} is 2.0. We set the path-average dispersion $\overline{\beta''} = -0.1$ $\mathrm{ps}^2/\mathrm{km} = 0.08$ ps/nm km, and the normalized path-average dispersion $\overline{D} = 1$.

In our first set of simulations, shown in Fig. 1, we chose the normalized dispersion in the two spans, $D_1 = 30$ and hence $D_2 = -28$. The parameter that we used to characterize the strength of the dispersion management is $\gamma = 2[(D_1 - \overline{D})L_1 - (D_2 - \overline{D})L_2]/t_{\mathrm{FWHM}}^2$, where L_1 and L_2 are the span lengths in the dispersion map. In this first set of simulations we found that γ is 2.9, corresponding to an energy-enhancement factor of 2.17. Figure 1 shows the timing jitter as a function of distance. We compared our Monte Carlo simulations with the timing jitter of the uniform-dispersion system divided by the square root of the enhancement factor, which we refer to as the modified Gordon–Haus timing jitter. In Refs. 2 and 3 it was predicted that the timing jitter would be reduced by the square root of the enhancement factor. We find that the timing jitter is reduced, but the reduction is less than predicted, and the deviation grows with the distance. Substituting the numerically determined stable pulse profile for $q(z, t)$ into Eq. (5), we also directly calculated the timing jitter. This semi-analytical calculation is in complete agreement with the Monte Carlo simulations. This result is highly significant because this approach yields greater precision than the Monte Carlo method at a fraction of the computational cost and is likely to have a wider applicability than just to this problem.

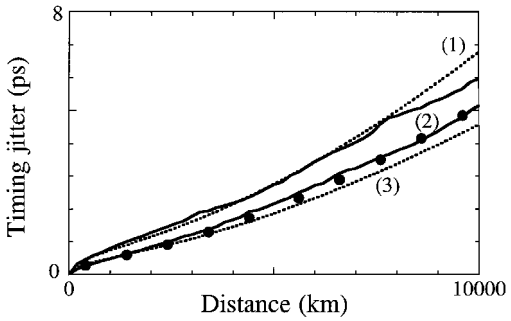

Fig. 1. Timing jitter as a function of distance with amplifiers spaced 50 km. Curves (1), timing jitter in a standard soliton system with uniform-dispersion fiber. Dashed curve, analytical result from Ref. 8; solid curve, the result of the average of 100 Monte Carlo simulations. Curve (2), timing jitter in a dispersion-managed soliton system. Circles, result of our semi-analytical approach; solid curve, result of the Monte Carlo simulations. Curve (3), modified Gordon–Haus result.

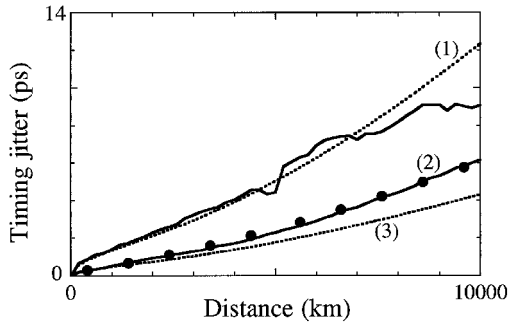

Fig. 2. Timing jitter as a function of distance with amplifiers spaced 100 km and placed at the points of maximum pulse expansion in the dispersion map. Curves (1)–(3) are as in Fig. 1.

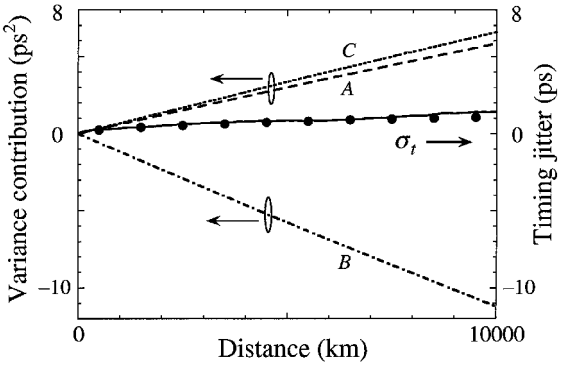

Fig. 3. Timing jitter as a function of distance with zero average dispersion. The solid curve and the circles are as in Fig. 1. A, B, and C are the results of Eqs. (6a), (6b), and (6c), respectively.

Figure 2 shows what happens when we locate the amplifiers at the points of greatest pulse expansion in the dispersion map and we increase the space between amplifiers to 100 km. Keeping $\overline{D}$ constant and $\gamma = 3.65$, we find that the deviation from the modified Gordon–Haus timing jitter differs by a large percentage, increasing to 30% after 10,000 km. The time–bandwidth product for this case is 0.66, and the enhancement factor equals 8.16. The pulse has a multipeaked structure. Extensive simulations show that as the time–bandwidth product increases, the predictions of the modified Gordon–Haus theory consistently become worse. This result is intuitively reasonable since the larger spectrum implies that the stable pulse can grab more noise. We also compared the results of Monte Carlo simulations with those from the Gordon–Haus theory in the uniform-dispersion fiber with the same path-average dispersion. We found that numerical simulations are consistent with the Gordon–Haus theory only within 8000 km in the case shown in Fig. 1. Beyond that distance, a considerable discrepancy between the Gordon–Haus theory and our simulations appears because linearization is no longer valid; in the case shown in Fig. 2 this discrepancy occurs even sooner. However, the linearization remains valid for the dispersion-managed solitons at up to 10,000 km because of their larger intensity.

Another interesting case that we calculated is the timing jitter in a system with zero average dispersion.[15,16] The results are shown in Fig. 3. We used a 100-km-long map with the amplifiers spaced 50 km apart and located at the edge of each span of the dispersion map. The normalized fiber dispersions were set at $D_1 = 90$ and $D_2 = -90$. In this case the terms B and C in Eq. (5) are comparable with the term A, and all of them grow linearly with distance. Since the contribution of the term B to the timing jitter is negative, we achieve a very small timing jitter at the end of a 10,000-km transmission line. The term A does not vanish because the independent, random noise contributions from the amplifiers at the beginning and in the middle of the map do not precisely cancel.

In conclusion, we have calculated the exact timing jitter for several different cases, using both a linearization approach and Monte Carlo simulations. We found that the deviation from the modified Gordon–Haus predictions, when they apply, can be significant. The linearization approach that we developed yields complete agreement with Monte Carlo simulations and higher precision at a fraction of the computational cost.

This study was supported by the National Science Foundation, the U.S. Department of Energy, and the U.S. Air Force Office of Scientific Research.

*Permanent address, Tyco Submarine Systems, 101 Crawford's Corner Road, Holmdel, New Jersey 07733-3030.

References

1. M. Suzuki, I. Morita, N. Edagawa, S. Yamamoto, H. Taga, and S. Akiba, Electron. Lett. **31,** 2027 (1995).
2. N. J. Smith, N. J. Doran, F. M. Knox, and W. Forysiak, Opt. Lett. **21,** 1981 (1996).
3. G. M. Carter, J. M. Jacob, C. R. Menyuk, E. A. Golovchenko, and A. N. Pilipetskii, Opt. Lett. **22,** 513 (1997).
4. M. Matsumoto and H. A. Haus, IEEE Photon. Technol. Lett. **9,** 785 (1997).
5. J. P. Gordon and H. A. Haus, Opt. Lett. **11,** 665 (1986).
6. N. J. Smith, W. Forysiak, and N. J. Doran, Electron. Lett. **32,** 2085 (1996).
7. T. Yu, E. A. Golovchenko, A. N. Pilipetskii, and C. R. Menyuk, Opt. Lett. **22,** 793 (1997).
8. D. Marcuse, J. Lightwave Technol. **9,** 505 (1991).
9. P. A. Humblet and M. Azizoglu, J. Lightwave Technol. **9,** 1576 (1991).
10. A. Mecozzi, J. Lightwave Technol. **12,** 1993 (1994).
11. M. Midrio, F. Matua, and M. Settembre, IEE Conf. Publ. (London) **48,** 315 (1997).
12. S. Kumar and F. Lederer, Opt. Lett. **22,** 1870 (1997).
13. T. Georges, F. Favre, and D. L. Guen, Inst. Electron. Inf. Commun. Eng. Trans. Electron. **E81-C,** 226 (1998).
14. H. A. Haus, J. Opt. Soc. Am. B **8,** 1122 (1991).
15. J. H. B. Nijhof, N. J. Doran, W. Forysiak, and F. M. Knox, Electron. Lett. **33,** 1726 (1997).
16. V. S. Grigoryan and C. R. Menyuk, Opt. Lett. **23,** 612 (1998).